

Dynamic Graph Convolution Network with Spatio-Temporal Attention Fusion for Traffic Flow Prediction

Xunlian Luo¹ Chunjiang Zhu² Detian Zhang¹ Qing Li³

Abstract

Accurate and real-time traffic state prediction is of great practical importance for urban traffic control and web mapping services (e.g. Google Maps). With the support of massive data, deep learning methods have shown their powerful capability in capturing the complex spatio-temporal patterns of road networks. However, existing approaches use independent components to model temporal and spatial dependencies and thus ignore the heterogeneous characteristics of traffic flow that vary with time and space. In this paper, we propose a novel dynamic graph convolution network with spatio-temporal attention fusion. The method not only captures local spatio-temporal information that changes over time, but also comprehensively models long-distance and multi-scale spatio-temporal patterns based on the fusion mechanism of temporal and spatial attention. This design idea can greatly improve the spatio-temporal perception of the model. We conduct extensive experiments in 4 real-world datasets to demonstrate that our model achieves state-of-the-art performance compared to 22 baseline models.

1. Introduction

In urban computing, popular web mapping services such as Google Maps, Bing Maps, and Baidu Maps heavily rely on accurate traffic flow prediction as a backend for their front-end applications such as personalized route planning and best/closest restaurant/gas station recommendation. Similarly, departments of transportation in next-generation smart cities often need to allocate traffic resources and optimize traffic control plans, e.g., for an exposition, by blocking a

¹Institute of Artificial Intelligence, Department of Computer Science and Technology, Soochow University, Suzhou, China. ²Department of Computer Science, University of North Carolina at Greensboro, Greensboro, NC, USA. ³Department of Computing, The Hong Kong Polytechnic University, Hong Kong, China. Correspondence to: Detian Zhang <detian@suda.edu.cn>.

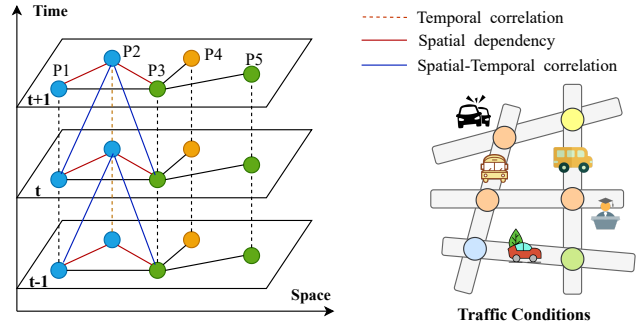


Figure 1. Complex spatio-temporal correlations

minimum number of streets while avoiding serious traffic congestion. The plan needs to be generated in advance and thus requires precise traffic flow estimation (Tedjopurnomo et al., 2020). Recently, we have witnessed the bloom of on-line ride-hailing/sharing services, e.g., Uber, Lyft, and Didi. They often provide functions to request a ride on the Web directly with no need to download apps. These Web-based services, again, need a powerful traffic prediction engine. A traffic flow prediction model analyzes large amounts of historical traffic data to estimate future traffic conditions based on statistical or data-driven methods. However, traffic flow is affected by complex spatial and temporal dependencies, which make accurate real-time traffic forecasting extremely challenging.

As shown in Fig. 1, traffic prediction differs from traditional time series analysis in that it is also influenced by spatial and many other external factors (Tedjopurnomo et al., 2020). In the temporal dimension, the overall traffic flow shows significant periodic patterns due to the travel routine of urban residents. Traffic flow also shows inevitable volatility due to external characteristics, e.g., graduation ceremonies and traffic accidents. The traffic information can be propagated in the spatial dimension with the road network topology. The traffic at a station is directly influenced by the vehicles passing upstream and downstream from the neighboring roads, which shows mobility and transience. Spatial and temporal correlations are also multi-scale, which can be roughly divided into global and local in space and long-term and short-term in time. In addition, the information propagation of the spatio-temporal graph occurs simultaneously in both time and space dimensions called spatio-temporal correlation, which has a significant impact on the change in

traffic flow.

Extensive research has been carried out to address these challenges. With the earliest work on time series modeling by building statistical models, such as VAR (Hamilton, 2020) and ARIMA (Kumar & Vanajakshi, 2015). These methods require data to satisfy specific stationarity assumptions and are not applicable to non-linearly varying traffic data. Later machine learning methods including SVR (Wu et al., 2004) and XGBoost (Dong et al., 2018) are used to capture nonlinear features of traffic flow. Machine learning models rely on manual processing of features, and it is difficult to fuse spatial information, so their ability to process features is limited. With the rapid development of deep neural network models, recurrent neural networks and variants such as LSTM (Hochreiter & Schmidhuber, 1997) and GRU (Chung et al., 2014) have good performance in modeling temporal sequence tasks. For traffic prediction, RNN models treat sequences of different roads as independent data streams, which only consider the temporal variability of data but ignore the spatial correlation. Graph neural networks proposed recently provide a feasible method for modeling non-Euclidean spatio-temporal networks. STGCN (Yu et al., 2018) proposes a full convolution spatio-temporal graph neural network for traffic prediction for the first time; T-GCN (Zhao et al., 2020) and DCRNN (Li et al., 2018) combine recurrent neural units with graph convolution networks to model spatio-temporal dependencies; GMAN (Zheng et al., 2020) mines the spatio-temporal characteristics of traffic data from the perspective of multi-attention mechanism; STGNN (Wang et al., 2020) introduces GRU and Transformer architectures to deal with local and global temporal dependencies. However, all of them rely on a priori knowledge of graph structure and fail to capture the dynamism and heterogeneity of spatio-temporal data. STSGCN (Song et al., 2020) proposes to construct local spatio-temporal graphs to learn spatial pattern information that changes dynamically over time, while it ignores the capture of effective temporal information. AGCRN (Bai et al., 2020) and DGCRN (Li et al., 2021) use adaptive graph generation with gated recurrent units to improve the representation of spatio-temporal heterogeneity, but do not pay enough attention to the global information. These methods have contributed to a tremendous improvement in the performance of traffic prediction from multiple perspectives, but they have not been combined in a cohesive way to address comprehensive features and their correlations.

To address the shortcomings of existing methods, in this paper, we propose a spatio-temporal Attention Fusion Dynamic Graph Convolution Network (AFDGCN) for traffic flow prediction. It employs feature augmentation, spatio-temporal synchronous recurrent networks with multiple attention fusion to capture complex traffic variation relationships from multi-scale spatio-temporal aspects. In summary,

the main contributions of this paper are:

- We propose an augmentation mechanism for enhancing the information interaction of spatio-temporal data in the feature channel and the temporal axis.
- We construct a dynamic graph convolution recurrent network for capturing local time dependence and spatial heterogeneity by coupling adaptive graph convolution with a gated recurrent unit structure, instead of using a separate network layer.
- We integrate temporal attention and spatial attention mechanisms to improve the model's ability to concentrate on the spatial field of view and long-distance information in complex scenes. This really reduces the model's error in long-distance prediction and enhances the robustness of the model.
- We conduct extensive experiments on 4 benchmark datasets, and evaluate the performance compared with 22 baseline methods. The results show that our proposed method outperforms all other methods in three standard evaluation metrics.

2. PROBLEM STATEMENT

Traffic flow prediction aims to use historical traffic observation data to predict the traffic flow changes in the future period under the topology of road networks. In a road network $G = (V, E, W)$, $V = \{v_1, v_2, \dots, v_N\}$ is the set of all monitoring points in the road network, E is the set of edges with each edge connecting two nodes in V . The connection relationship of these edges can be expressed as a symmetric adjacency matrix $W \in R^{N \times N}$, where the i, j -th element $W[i, j]$ represents the strength of the connection between node v_i and node v_j . The distance-based weighted adjacency matrix W can be formulated using the radial basis function (RBF) kernel:

$$w_{i,j} = \begin{cases} \exp(-\frac{d_{i,j}^2}{\sigma^2}), & i \neq j \text{ and } \exp(-\frac{d_{i,j}^2}{\sigma^2}) \geq \epsilon \\ 0, & \text{otherwise} \end{cases} \quad (1)$$

where $w_{i,j}$ denotes the edge weights of the adjacency matrix, which are determined by the actual distance between node i and node j in the road network geography. σ^2 and ϵ are used to control the sparsity of the weight matrix W . Graph signal matrix $X_t \in R^{N \times C}$ is the attribute features of all nodes in the graph at time step t , where C is the number of node attribute features, which generally refers to features such as traffic flow, speed or volume. We denote all node signals in a graph at time interval T as $X \in R^{T \times N \times C}$. The traffic prediction problem can be formally defined as:

$$[X_{t+1}, \dots, X_{t+Q}] = f_{\Theta}(G; (X_{t-P}, \dots, X_{t-1}, X_t)) \quad (2)$$

where the prediction model is abstractly represented as a learnable mapping function f based on a parameter matrix Θ , P is the length of a given historical time series, and Q is the length of the future time series predicted by the model.

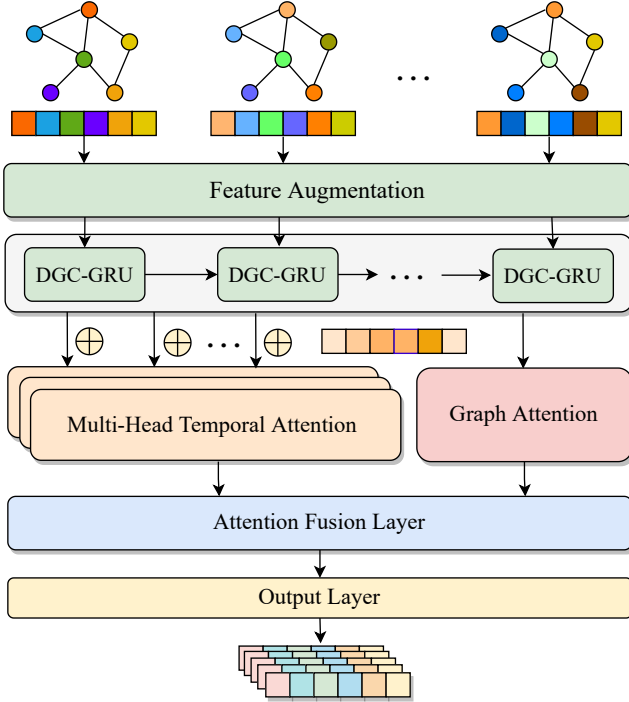


Figure 2. Model Overview of Dynamic Graph Convolution Network with Spatio-Temporal Attention Fusion

3. Methodology

We design a novel graph neural network AFDGCN that consists of four modules, namely feature augmentation, dynamic graph convolution recurrent network, multi-head temporal attention, and graph attention. Fig. 2 plots the network architecture of our model, AFDGCN.

3.1. Feature Augmentation Module

Due to the correlation between multiple features of traffic data, different features have different influences or contributions to traffic flow prediction. In order to fully understand the intrinsic characteristics of time series data, we develop a feature augmentation layer inspired by the channel attention mechanism (Woo et al., 2018), which amplifies the interaction of global feature dimensions to help the model automatically learn the importance of different features. The feature augmentation layer is based on a “squeeze-excitation” structure (Liu et al., 2021). On the one hand, it incorporates features at different scales, and on the other hand, it automatically calibrates the contributions of different feature channels, which helps to improve the representation of the feature map.

The feature augmentation layer consists of two submodules, namely channel attention and temporal attention. The channel attention submodule is a two-layer multilayer perceptron, which first performs a squeezing operation on the input feature map. This helps the model recalibrate the fea-

tures with a low-dimensional distribution. It then analyzes the influence of each channel through a single activation process and a self-threshold mechanism. To focus on the structural information of the time series (important time points), the temporal submodule uses two one-dimensional convolution layers for temporal feature fusion, which are processed in a similar way to channel attention. The two structures are concatenated to enhance the information interaction of spatio-temporal data in the feature channel and temporal dimensions.

Given the input feature map $X_1 \in R^{T \times N \times C}$, the channel attention submodule can be formulated as:

$$X_2 = \sigma(W_2 \chi(W_1 X_1 + b_1) + b_2) \odot X_1 \quad (3)$$

where \odot is the element-wise product, χ is the ReLU activation function, σ is the sigmoid activation function, and W_1, W_2 and b_1, b_2 are the weight parameters and bias of the fully connected layer, respectively. After the channel attention processing and dimensional transformation, the feature map $X_2 \in R^{T \times N \times C}$ serves as input to the temporal submodule as:

$$X_3 = \sigma(\Theta_{1,k} \star \chi(\Theta_{1,k} \star X_2(t)) \odot X_2(t), \quad (4)$$

where $\Theta_{1,k}$ is the convolution kernel. After preprocessing, the reweighted feature maps are used as the output of the feature augmentation module to feed in the training of the subsequent structures.

3.2. Dynamic Graph Convolution Recurrent Network

Traffic network G can be naturally encoded as a topological graph composed of nodes and edges, and the propagation of interconnected roads along with traffic flow is often highly correlated. In order to capture the potential spatial correlation in traffic data, we use a graph convolution neural network to simulate the information propagation process of dynamic spatial structure (Jiang & Luo, 2022), extracting the feature representation of the nodes. Let $A \in R^{N \times N}$ denote the adjacency matrix of the graph, I_N denote an identity matrix, and $D \in R^{N \times N}$ denote the degree matrix of nodes, which is a diagonal matrix recording the number of connected edges of each node. $\tilde{A} = D^{-\frac{1}{2}} A D^{-\frac{1}{2}}$ denotes normalized adjacency matrix. $X \in R^{N \times C}$ is the input graph signal, $Z \in R^{N \times F}$ represents the output signal of the graph convolution operation, and $W \in R^{C \times F}$ and $b \in R^F$ are the learnable parameters of the model. The first-order Chebyshev graph convolution network (Kipf & Welling, 2016) is defined as:

$$Z = (I_N + D^{-\frac{1}{2}} A D^{-\frac{1}{2}}) X W + b. \quad (5)$$

Although it is useful for aggregating spatial information of neighboring roads, the dynamic adaptation of time series

with nodes' own factors (e.g., POIs, road structures, and road types) can also have a significant impact on traffic. A uniform feature aggregation approach for all nodes cannot obtain accurate prediction results; the unique pattern information of each node should be taken into account, instead of only a single geographical distance. A dynamic graph generation approach can make full use of the spatial properties of traffic data and get rid of the limitations of static graph convolution.

We propose a graph convolution method based on parameter learning for node embedding with **dynamic generation of the adjacency matrix**. It considers the spatial heterogeneity of different nodes in the road network and enables the model to mine the abstract spatial representation from end-to-end training. We predefine the embedding vector $E_G \in R^{N \times d}$ for all nodes, where d denotes the embedding dimension and $d \ll N$. We then infer the hidden correlation between nodes by $E_G \cdot E_G^T \in R^{N \times N}$ to avoid directly defining the adaptive parameter matrix $A_G \in R^{N \times N}$ with too many parameters. Then $E_G \cdot E_G^T$ is processed by the softmax function to obtain the normalized adjacency matrix. This formula is defined as:

$$\tilde{A} = D^{-\frac{1}{2}} A D^{-\frac{1}{2}} = \text{softmax}(\text{ReLU}(E_G \cdot E_G^T)), \quad (6)$$

where E_G will be iteratively updated during the training process to understand the hidden dependencies between different traffic sequences, and the hyperparameter d is used to represent the spatial dimensionality of node learning.

We observe that the weight coefficient and bias used by the traditional GCN for feature linear transformation are shared by all nodes. This ignores the differences in traffic patterns among nodes and limits the capability of feature processing. However, assigning independent parameters $W_G \in R^{N \times C \times F}$ to each node could result in a very large number of parameters for the model that cannot be optimized properly. Inspired by the matrix decomposition, we perform matrix multiplication of $W_G \in R^{d \times C \times F}$ ($b_G \in R^{d \times F}$) with the node embedding $E_G \in R^{N \times d}$ to generate new model parameters $W = E_G W_G$ ($b = E_G b_G$, respectively). In this way, the dynamic graph convolution network is defined as:

$$Z = (I_N + \text{softmax}(\text{ReLU}(E_G \cdot E_G^T))) X E_G W_G + E_G b_G. \quad (7)$$

To capture both temporal and spatial dependencies of the traffic data, we couple the gated recurrent unit (GRU) with **dynamic graph generation** to obtain a dynamic graph convolution recurrent network (DGC-GRU) module, which takes advantage of the information transmission between GRUs to capture the spatio-temporal heterogeneity of the dynamics of the sequence data at each time step. Due to the superior performance of GRU in processing sequential tasks, we embed graph convolution operations in the original GRU

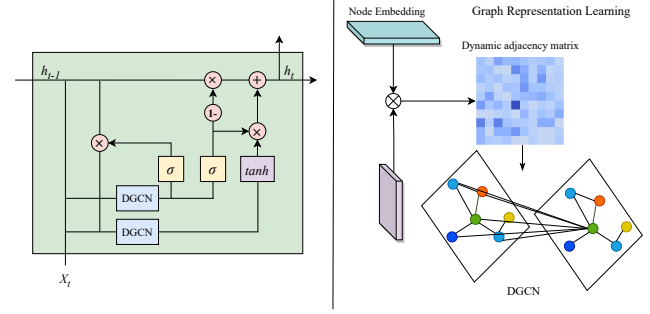


Figure 3. Dynamic Graph Convolution Recurrent Network

structure to capture sequential information while merging spatial relationships, as shown in Fig. 3. In addition to the present data input, each time step receives a hidden representation from the previous time step, which is used to control the memory and forgetting of information. Here, the GRU operation is applied to each node in the graph, and the parameters are shared with each other. Specifically, given the previously hidden representation H_{t-1} and the input data $X_{:,t}$ at time point t , we represent the computation of a single-step gated recurrent unit as:

$$\begin{aligned} z_t &= \sigma(\tilde{A}[X_{:,t}, H_{t-1}]W_z + b_z) \\ r_t &= \sigma(\tilde{A}[X_{:,t}, H_{t-1}]W_r + b_r) \\ \hat{H}_t &= \tanh(\tilde{A}[X_{:,t}, r \odot H_{t-1}]W_{\hat{h}} + Eb_{\hat{h}}) \\ H_t &= z \odot H_{t-1} + (1 - z) \odot \hat{H}_t, \end{aligned} \quad (8)$$

where $W_z, b_z, W_r, b_r, W_{\hat{h}}$, and $b_{\hat{h}}$ are learnable parameters of the recurrent network layer and H_t is the output of the current time step t .

The DGCN adopts a **dynamic graph generation** strategy with parameter learning to exploit spatially heterogeneous information without introducing external data. The combination of dynamic graph convolution network and GRUs can fuse the spatio-temporal dependencies of each stage and enhance the model's ability to handle fine-grained spatio-temporal patterns. However, GRU does not rigidly memorize all fixed-length sequences, but selectively stores information of historical time steps through hidden states. Although it can effectively capture local temporal information from traffic sequence data, it is insensitive to long-distance temporal relationships due to the forgetting characteristic of gating and the direction of information propagation.

3.3. Multi-head Temporal Attention Layer

In the temporal dimension of traffic data, the traffic state in the current time period of a spatial region is highly correlated with those of the time period before and after the present time in the same region. To further capture the long-term pattern of traffic data, we design a multi-head temporal attention layer to model the global contextual information

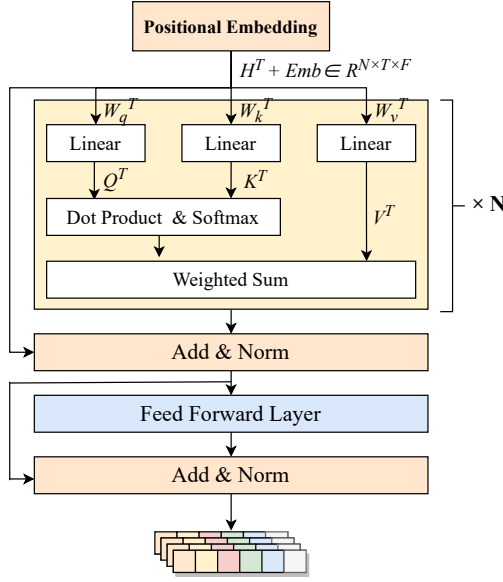


Figure 4. Multi-head Temporal Attention Layer

of the sequence. The layer consists of a positional embedding, a multi-head attention mechanism, and a feedforward network layer, as shown in Fig. 4. The temporal attention mechanism enables the model to observe longer-term temporal trends and focus on highly correlated information to compensate for the deficiencies of GRU in modeling temporal dependence.

The sequence of features $\{H_1[i, :], H_2[i, :], \dots, H_T[i, :]\}$ output by the DGC-GRU module is fed into the temporal attention module. Considering that the multi-head attention mechanism (Vaswani et al., 2017) ignores the relative positions in the sequence during the dot product operation, we first add a position vector to the input data at each moment. That is,

$$\hat{H}_t[i, :] = H_t[i, :] + e_t, \quad (9)$$

where the position encoding token e_t is defined as:

$$e_t = \begin{cases} \sin(t/10000^{2i/d_{model}}), & \text{if } t = 0, 2, 4, \dots \\ \cos(t/10000^{2i/d_{model}}), & \text{otherwise} \end{cases} \quad (10)$$

The encoded input sequence $\hat{H} \in R^{N \times T \times F}$ is used to generate the query matrix Q , key matrix K , and value matrix V of the self-attention mechanism as shown in Eq. (11). Then Q and K^T are multiplied and normalized to obtain the weight coefficients of the sequence in the time dimension. Finally, the weight coefficients are superimposed on V to obtain the weighted results for different time steps. Formally, we have that:

$$Q = \hat{H}W_q^T, K = \hat{H}W_k^T, V = \hat{H}W_v^T \quad (11)$$

$$Attention(Q, K, V) = softmax\left(\frac{QK^T}{\sqrt{d_k}}\right)V, \quad (12)$$

where W_q^T , W_k^T , and W_v^T are the projection matrix to be learned, $\sqrt{d_k}$ is the weight scaled factor, and the softmax function is used to normalize the attention scores to obtain the weight distribution of each value.

We employ the multi-head attention mechanism because it allows the model to jointly focus on features from different representation subspaces at different positions such that, each head captures different semantic information and improves the model's ability to perceive global temporal relationships (Zheng et al., 2020). In the multi-head attention mechanism, multiple sets of self-attentions are applied in the original input sequence and then their results are concatenated. After that, the concatenated result after a linear transformation is used as the output of the multi-head attention mechanism. The mathematical formula is defined as:

$$MultiHead(Q, K, V) = Concat(head_1, head_2, \dots, head_n)W^O, \\ head_i = Attention(\hat{H}W_i^Q, \hat{H}W_i^K, \hat{H}W_i^V). \quad (13)$$

Here W^O is the projection matrix of the linear transformation. Finally, the output of the multi-head temporal attention layer H_T is passed into the feedforward network layer with a residual connection and layer normalization after each sub-layer.

3.4. Graph Attention Module

Adaptive dynamic graph convolution can capture the heterogeneity and local space information, but the spatial information of the traffic environment is often irregular and dynamically changing. To see this, on the one hand, a major event (e.g., concerts, traffic construction) at a location provokes a sudden increase or decrease of traffic in the neighboring area. On the other hand, vehicles can reach their destinations by following different paths in a road network. In order to capture this complex and varying spatial pattern, our model applies a graph attention network module. The graph attention network (Velickovic et al., 2017) is an effective neural network that dynamically assigns different weights to the neighboring vertex features when they are aggregated toward the center according to the traffic characteristics of the center and neighboring vertices.

The input of the graph attention layer is the set of all node feature vectors: $H^{l-1} = \{h_1, h_2, \dots, h_N\}$, and the output is the set of all node hidden layer representations: $H^l = \{h'_1, h'_2, \dots, h'_n\}$. In calculating the attention coefficient α_{ij} between node i and node j , we first apply a linear transformation in the features of the two nodes and then concatenate and map the feature vectors into attention values. Formally, the computation is:

$$e_{ij} = a(Wh_i, Wh_j), j \in N_i, \quad (14)$$

where N_i is the set of neighboring nodes of node i , a is

the learnable parameter of the linear layer. The correlation score between node i and node j is then activated by the LeakyReLU function and normalized over all neighboring nodes of i using the softmax function to obtain the normalized attention coefficient. The calculation is formally expressed as:

$$\alpha_{ij} = \text{softmax}(e_{ij}) = \frac{\exp(\text{LeakyReLU}(e_{ij}))}{\sum_{k \in N_i} \exp(\text{LeakyReLU}(e_{ik}))}. \quad (15)$$

The feature aggregation is performed for every node to get its output feature representation:

$$h'_i = \sigma\left(\sum_{j \in N_i} \alpha_{ij} W h_j\right). \quad (16)$$

Here we write the calculation process of the graph attention module in the form of matrix operations, expressed as follows:

$$H^l = (M \odot A) H^{l-1} W. \quad (17)$$

where A is a static matrix calculated from the distance (1), the elements in $M \in R^{N \times N}$ are the dynamic attention coefficients. W is the weight parameter that can be learned. H^l indicates the output of the module. We use linear summation operations to fuse temporal and graph attention, thus reducing the computational overhead of our model. But one can choose a different fusing method to potentially improve the prediction performance in practice. Finally, we map the fused hidden representation to the prediction space.

4. Experiment

4.1. Experimental Settings

Dataset. We use commonly used real-world traffic flow data collected by the California Department of Transportation at highway sensors (Chen et al., 2001), including PeMSD3, PeMSD4, PeMSD7, and PeMSD8. They record traffic information such as flow, speed, and occupancy, with a sampling interval of 5 minutes between two data versions. Details of the dataset statistics are provided in Table 1.

The raw data are uniformly standardized using Z-Score (Song et al., 2020) and then divided into the training set, validation set, and test set with a ratio of 6 : 2 : 2. The training set is disrupted before training and the validation set is used to control the early stopping of the training process. In the multi-step prediction task, we set both the input sequence P and the output sequence Q to 12.

Baseline Methods. To verify the effectiveness of the proposed model, we compare it with different methods including traditional statistical methods, deep learning methods,

Table 1. The statistics of the tested real-world datasets

Dataset	Sensors	Time Steps	Time Range
PeMSD3	358	26,208	Sept - Nov, 2018
PeMSD4	307	16,992	Jan - Feb, 2018
PeMSD7	883	28,224	May - Aug, 2017
PeMSD8	170	17,856	Jul - Aug, 2016

and graph neural network methods. In total, we use 22 baseline models with key baselines briefly described below:

- **ARIMA** (Kumar & Vanajakshi, 2015): Auto-regressive Integrated Moving Average with Kalman filter is a widely used statistical model for time series.
- **VAR** (Wu et al., 2004): Vector Auto-Regression assumes that the historical time series is stationary and forecasts by estimating the relationship between the time series and its lagged values.
- **FC-LSTM** (Sutskever et al., 2014): A recurrent neural network with fully connected LSTM hidden units.
- **TCN** (Bai et al., 2018): A layer-by-layer stacked temporal causal convolution with exponentially increasing expansion factors.
- **STGCN** (Yu et al., 2018): Combining Chebyshev graph convolution with 1D temporal convolution to construct a fully convolution spatio-temporal network.
- **DCRNN** (Li et al., 2018): Combining Bi-Directional diffusion of graph convolution with recurrent neural networks, and using an Encoder-Decoder architecture.
- **AGCRN** (Bai et al., 2020): Adopting a Data Adaptive Graph Generation module to automatically infer the dependencies between different traffic sequences and capture dynamic spatial and temporal correlations.
- **Z-GCNETs** (Chen et al., 2021): Augmenting the DL architecture with the most important time-conditional topological information of the data and introducing the concept of jagged persistence in the time-aware graph convolution network.
- **STG-NCDE** (Choi et al., 2022): Integrating graph convolution networks and neural control differential equations for the processing of spatio-temporal sequences.

Throughout the experiments, we use three evaluation metrics, MAE, RMSE, and MAPE (which are defined in the Appendix), to compare the overall performance of different models on the test datasets.

Parameters Setup. Recalling that the task is to learn a mapping function $f : R^{T \times N \times C} \rightarrow R^{T' \times N \times C}$. Our aim is to predict the traffic state in the next hour based on the historical traffic data of the previous hour, i.e. $T = T' = 12$. In our experiments, we set all the hidden dimensions to 64 and the head of attention to 4. Both the number of layers in recurrent neural network and the attention are 1. We use the Adam (Kingma & Ba, 2015) optimizer for training

Table 2. Performance comparison of AFDGCN and other baseline models. AFDGCN achieves the best performance for all datasets.

Model	PEMSD3			PEMSD4			PEMSD7			PEMSD8		
	MAE	RMSE	MAPE	MAE	RMSE	MAPE	MAE	RMSE	MAPE	MAE	RMSE	MAPE
HA	31.58	52.39	33.78%	38.03	59.24	27.88%	45.12	65.64	24.51%	34.86	59.24	27.88%
ARIMA	35.41	47.59	33.78%	33.73	48.80	24.18%	38.17	59.27	19.46%	31.09	44.32	22.73%
VAR	23.65	38.26	24.51%	24.54	38.61	17.24%	50.22	75.63	32.22%	19.19	29.81	13.10%
FC-LSTM	21.33	35.11	23.33%	26.77	40.65	18.23%	29.98	45.94	13.20%	23.09	35.17	14.99%
TCN	19.32	33.55	19.93%	23.22	37.26	15.59%	32.72	42.23	14.26%	22.72	35.79	14.03%
STGCN	17.55	30.42	17.34%	21.16	34.89	13.83%	25.33	39.34	11.21%	17.50	27.09	11.29%
DCRNN	17.99	30.31	18.34%	21.22	33.44	14.17%	25.22	38.61	11.82%	16.82	26.36	10.92%
Graph WaveNet	19.12	32.77	18.89%	24.89	39.66	17.29%	26.39	41.50	11.97%	18.28	30.05	12.15%
ASTGCN	17.34	29.56	17.21%	22.93	35.22	16.56%	24.01	37.87	10.73%	18.25	28.06	11.64%
STSGCN	17.48	29.21	16.78%	21.19	33.65	13.90%	24.26	39.03	10.21%	17.13	26.80	10.96%
AGCRN	15.98	28.25	15.23%	19.83	32.26	12.97%	22.37	36.55	9.12%	15.95	25.22	10.09%
STGODE	16.50	27.84	16.69%	20.84	32.82	13.77%	22.59	37.54	10.14%	16.81	25.97	10.62%
Z-GCNETs	16.64	28.15	16.39%	19.50	31.61	12.78%	21.77	35.17	9.25%	15.67	25.11	10.01%
STG-NCDE	<u>15.57</u>	<u>27.09</u>	15.06%	<u>19.21</u>	<u>31.09</u>	12.76%	<u>20.53</u>	<u>33.84</u>	<u>8.80%</u>	<u>15.45</u>	24.81	<u>9.92%</u>
DSTAGNN	<u>15.57</u>	27.21	<u>14.68%</u>	19.30	31.46	<u>12.70%</u>	21.67	34.51	9.01%	15.67	<u>24.77</u>	9.94%
AFDGCN	14.97	25.81	14.18%	19.09	31.01	12.62%	20.22	33.80	8.52%	15.02	24.37	9.68%

the model. We select Huber Loss (Huber, 1992) as the loss function. The batch size of the data is 64, the number of epochs is 300, and the initialized learning rate is 0.003. An early stopping strategy is used with a patience of 15 iterations on the validation dataset.

4.2. Experiment Results

Table 2 presents the evaluation results of AFDGCN and major baseline methods on the four tested datasets. The additional table can be found in the Appendix. The bold values and the underlined values are the best and second-best prediction performances, respectively. Our method (AFDGCN) always achieves the best performance and is in bold. Compared with the best baseline (underlined), the performance of AFDGCN on four datasets (PeMSD3, PeMSD4, PeMSD7, and PeMSD8) is improved by 3.85%, 0.62%, 1.51%, and 2.78% on MAE and 3.41%, 0.63%, 3.50%, and 2.42% on MAPE respectively. In particular, the improvements are more significant for the PeMSD3 and PeMSD8 datasets.

We observe that statistical methods such as HA, ARIMA, and VAR have difficulty in handling nonlinear, non-stationary time series data and the model prediction errors are high. Although deep learning methods such as FC-LSTM and TCN have advantages over statistical models, they only consider temporal correlations and cannot exploit spatial dependencies, thus having a limited ability to model spatial-temporal data. Spatio-temporal graph networks such as STGCN, DCRNN, and Graph WaveNet are designed with spatio-temporal components, so they generally have better performance compared with temporal-only-based methods. AGCRN and STGODE are free from the limitation of fixed graph structure and use self-adaptive or dynamic properties

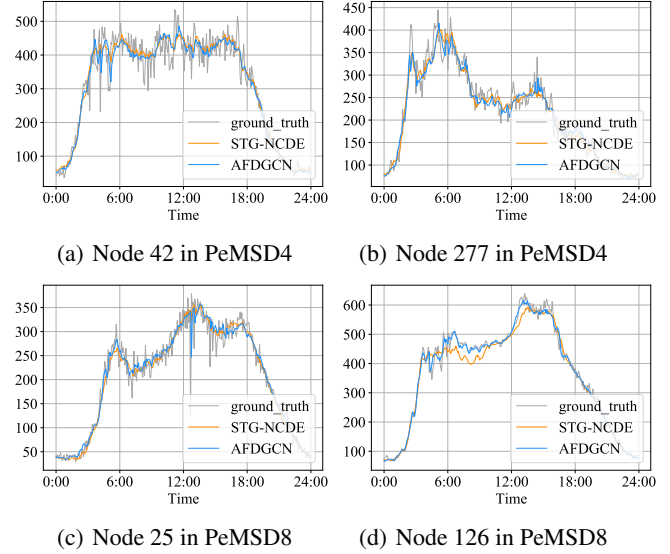


Figure 5. Traffic forecasting at different time points

of spatial association between nodes in historical data to construct the graph structure. They further improve the prediction performance compared with the previous methods. In contrast, our method not only considers the effects of spatio-temporal correlation but also mines the multi-scale and long-distance traffic fluctuation relationships from the perspective of spatio-temporal attention.

Furthermore, we quantify the difference between our model and the best baseline model using the relative error rate. Across the four datasets, the average MAE, RMSE, and MAPE values for AFDGCN are 17.33, 28.75, and 11.25%, respectively; the corresponding average values of DSTAGNN (Lan et al., 2022) are 18.05 (104.2%), 29.48 (102.5%), and 11.58% (103.0%), and the average error performance of STG-NCDE (Choi et al., 2022) are 17.69 (102.1%), 29.21 (101.6%) and 11.64% (103.5%). Taken

together, the improved gain of our model compared to these two models ranges from 1.6% to 4.2%.

To clearly examine the difference in prediction performance between our method and the baseline methods, we plot in Fig. 5 the predicted and ground truth of our method (AFDGCN) versus STG-NCDE for several stations/nodes within a given day. Node 42 and 277 (and Node 25 and 126) are the two regions with the highest traffic fluctuations in PeMSD4 (and PeMSD8, respectively). AFDGCN and STG-NCDE well fit the real conditions of traffic variations in many time periods, but our method shows more accurate prediction performance in challenging traffic scenarios, e.g., during traffic peak hours or when the magnitude of fluctuations is drastic. In particular, our method adapts well to changes in traffic trends, e.g., 4-6 and 11-12 in (a), 4-6 and 14-15 in (b), 4-6 and in (c), and 4-15 in (d). In contrast, the prediction curves of STG-NCDE significantly deviate from the ground truth because of its limited predictive power.

Table 3. The training and inference time in PEMS4 dataset under a Tesla V100 GPU(s/epoch)

Model	Params	Training(s)	Inference(s)
DSTAGNN	3,579,728	134.72	14.94
STG-NCDE	322,588	92.04	10.94
STGODE	714,504	57.38	7.27
AGCRN	748,810	21.68	2.88
AFDGCN	435,121	25.17	2.61

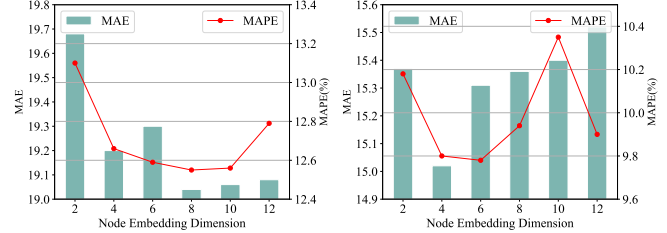
4.3. Additional Experimental Studies

Efficiency study. We first compare the computational cost of our model AFDGCN with several competitive baseline models on the PEMS4 dataset using the same hardware NVIDIA Tesla V100. As shown in Table 3, AFDGCN has a comparable training and inference time as AGCRN but attains much better predictive performance. Compared with STGODE, the training time and inference time of AFDGCN are reduced by 56.13% and 64.10%. Although STG-NCDE has fewer parameters than AFDGCN, the complex model structure and operators make the computational cost of STG-NCDE significantly higher than AFDGCN. The training time and inference time of AFDGCN are 4-5x and 4-6x faster than DSTAGNN and STG-NCDE, respectively. Remarkably, our model outperforms all the baseline methods in the predictive performance by only using highly competitive training and inference time.

Ablation study. We perform an ablation study on different modules of our model to investigate their individual contributions in the PeMSD4 and PeMSD8 datasets. Let DGCGRU denote the dynamic graph convolution recurrent network, and DGC-ATT denote DGCGRU with multi-head temporal attention. We denote the full model AFDGCN with feature augmentation removed and AFDGCN with graph attention layer removed as w/o FA and w/o GAT, respec-

Table 4. The results of an ablation study in AFDGCN

Module	PEMSD4			PEMSD8		
	MAE	RMSE	MAPE	MAE	RMSE	MAPE
DGCGRU	19.80	32.20	13.18%	16.01	25.51	10.35%
DGCGRU with ATT	19.32	31.87	12.79%	15.53	24.91	10.01%
AFDGCN w/o FA	19.11	31.65	12.67%	15.35	24.49	9.98%
AFDGCN w/o GAT	19.11	31.48	12.61%	15.29	24.68	9.71%
AFDGCN	19.04	31.11	12.55%	15.02	24.36	9.80%



(a) Embedding in PeMSD4 (b) Embedding in PeMSD8

Figure 6. The Effects of the Embedding Dimension

tively. The prediction results of these methods for PeMSD4 and PeMSD8 are summarized in Table 4. DGCGRU performs normally as expected. After adding the multi-headed temporal attention mechanism, (DGC-ATT)DGCGRU with ATT achieves significant improvements in the three evaluation metrics. This demonstrates the effectiveness of the temporal attention mechanism in modeling global temporal dependence. In addition, AFDGCN with either the feature-enhanced layer or the graph attention layer removed has a noticeable loss in the prediction performance.

Hyperparametric study. An essential parameter in AFDGCN is the node embedding size, which not only affects the quality of the learning graph but also determines the diversity of parameters in the DGCGRU layer. Figures 6(a) and 6(b) show the effects of different node embedding dimensions on the model prediction results. It can be seen that the optimal node embedding dimensions for the PeMSD4 and PeMSD8 datasets are 8 and 4, respectively. On the one hand, a node embedding with a larger dimension contains more parameter information, which improves the expressiveness of the model to infer more complete spatial correlations. On the other hand, the number of parameters is larger, which results in a model prone to overfitting.

5. Conclusion

In this paper, we propose a novel dynamic spatio-temporal graph neural network model for traffic prediction tasks. Our model fuses gated recurrent networks with adaptive dynamic graph convolution with the aim of capturing dynamic spatio-temporal correlations. We show that fusing spatio-temporal attention mechanisms can improve prediction accuracy in complex scenarios. We conduct experiments in 4 publicly available traffic datasets, and the results demonstrate the effectiveness and superiority of AFDGCN.

References

- Abu-El-Haija, S., Perozzi, B., Kapoor, A., Alipourfard, N., Lerman, K., Harutyunyan, H., Steeg, G. V., and Galstyan, A. Mixhop: Higher-order graph convolutional architectures via sparsified neighborhood mixing. In *Proceedings of the 36th International Conference on Machine Learning, ICML 2019, 9-15 June 2019, Long Beach, California, USA*, 2019.
- Bai, L., Yao, L., Li, C., Wang, X., and Wang, C. Adaptive graph convolutional recurrent network for traffic forecasting. In *Advances in Neural Information Processing Systems*, 2020.
- Bai, S., Kolter, J. Z., and Koltun, V. An empirical evaluation of generic convolutional and recurrent networks for sequence modeling. *arXiv preprint*, arXiv:1803.01271, 2018.
- Chen, C., Petty, K., Skabardonis, A., Varaiya, P., and Jia, Z. Freeway performance measurement system: mining loop detector data. *Transportation Research Record*, pp. 96–102, 2001.
- Chen, W., Chen, L., Xie, Y., Cao, W., Gao, Y., and Feng, X. Multi-range attentive bicomponent graph convolutional network for traffic forecasting. In *Proceedings of the AAAI conference on artificial intelligence*, pp. 3529–3536, 2020.
- Chen, Y., Segovia, I., and Gel, Y. R. Z-gcnets: time zigzags at graph convolutional networks for time series forecasting. In *International Conference on Machine Learning*, pp. 1684–1694, 2021.
- Choi, J., Choi, H., Hwang, J., and Park, N. Graph neural controlled differential equations for traffic forecasting. In *Proceedings of the AAAI Conference on Artificial Intelligence*, pp. 6367–6374, 2022.
- Chung, J., Gülçehre, Ç., Cho, K., and Bengio, Y. Empirical evaluation of gated recurrent neural networks on sequence modeling. *arXiv preprint arXiv:1412.3555*, 2014.
- Dong, X., Lei, T., Jin, S., and Hou, Z. Short-term traffic flow prediction based on xgboost. In *2018 IEEE 7th Data Driven Control and Learning Systems Conference*, pp. 854–859, 2018.
- Fang, Z., Long, Q., Song, G., and Xie, K. Spatial-temporal graph ode networks for traffic flow forecasting. In *Proceedings of the 27th ACM SIGKDD Conference on Knowledge Discovery & Data Mining*, pp. 364–373, 2021.
- Guo, S., Lin, Y., Feng, N., Song, C., and Wan, H. Attention based spatial-temporal graph convolutional networks for traffic flow forecasting. In *Proceedings of the AAAI conference on artificial intelligence*, pp. 922–929, 2019a.
- Guo, S., Lin, Y., Li, S., Chen, Z., and Wan, H. Deep spatial-temporal 3d convolutional neural networks for traffic data forecasting. *IEEE Trans. Intell. Transp.*, pp. 3913–3926, 2019b.
- Guo, S., Lin, Y., Wan, H., Li, X., and Cong, G. Learning dynamics and heterogeneity of spatial-temporal graph data for traffic forecasting. *IEEE Transactions on Knowledge and Data Engineering*, 2021.
- Hamilton, J. D. *Time series analysis*. Princeton university press, 2020.
- Han, L., Du, B., Sun, L., Fu, Y., Lv, Y., and Xiong, H. Dynamic and multi-faceted spatio-temporal deep learning for traffic speed forecasting. In *KDD '21: The 27th ACM SIGKDD Conference on Knowledge Discovery and Data Mining*, 2021a.
- Han, L., Du, B., Sun, L., Fu, Y., Lv, Y., and Xiong, H. Dynamic and multi-faceted spatio-temporal deep learning for traffic speed forecasting. In *Proceedings of the 27th ACM SIGKDD Conference on Knowledge Discovery & Data Mining*, pp. 547–555, 2021b.
- Hochreiter, S. and Schmidhuber, J. Long short-term memory. *Neural computation*, pp. 1735–1780, 1997.
- Huang, R., Huang, C., Liu, Y., Dai, G., and Kong, W. Lsgcn: Long short-term traffic prediction with graph convolutional networks. In *IJCAI*, pp. 2355–2361, 2020.
- Huber, P. J. Robust estimation of a location parameter. In *Breakthroughs in statistics*, pp. 492–518, 1992.
- Jiang, W. and Luo, J. Graph neural network for traffic forecasting: A survey. *Expert Systems with Applications*, pp. 117921, 2022.
- Kieu, T., Yang, B., Guo, C., and Jensen, C. S. Outlier detection for time series with recurrent autoencoder ensembles. In *IJCAI*, pp. 2725–2732, 2019.
- Kingma, D. P. and Ba, J. Adam: A method for stochastic optimization. In *3rd International Conference on Learning Representations, ICLR 2015, San Diego, CA, USA, May 7-9, 2015, Conference Track Proceedings*, 2015.
- Kipf, T. N. and Welling, M. Semi-supervised classification with graph convolutional networks. *arXiv preprint arXiv:1609.02907*, 2016.
- Kumar, S. V. and Vanajakshi, L. Short-term traffic flow prediction using seasonal arima model with limited input data. *European Transport Research Review*, pp. 1–9, 2015.

- Lan, S., Ma, Y., Huang, W., Wang, W., Yang, H., and Li, P. Dstagnn: Dynamic spatial-temporal aware graph neural network for traffic flow forecasting. In *International Conference on Machine Learning*, pp. 11906–11917, 2022.
- Li, F., Feng, J., Yan, H., Jin, G., Yang, F., Sun, F., Jin, D., and Li, Y. Dynamic graph convolutional recurrent network for traffic prediction: Benchmark and solution. *ACM Transactions on Knowledge Discovery from Data (TKDD)*, 2021.
- Li, Y., Yu, R., Shahabi, C., and Liu, Y. Diffusion convolutional recurrent neural network: Data-driven traffic forecasting. In *6th International Conference on Learning Representations*, 2018.
- Lin, Z., Feng, J., Lu, Z., Li, Y., and Jin, D. Deepstn+: Context-aware spatial-temporal neural network for crowd flow prediction in metropolis. In *Proceedings of the AAAI conference on artificial intelligence*, pp. 1020–1027, 2019.
- Liu, Y., Shao, Z., and Hoffmann, N. Global attention mechanism: Retain information to enhance channel-spatial interactions. *CoRR*, abs/2112.05561, 2021. URL <https://arxiv.org/abs/2112.05561>.
- Park, C., Lee, C., Bahng, H., Tae, Y., Jin, S., Kim, K., Ko, S., and Choo, J. St-grat: A novel spatio-temporal graph attention networks for accurately forecasting dynamically changing road speed. In *Proceedings of the 29th ACM international conference on information & knowledge management*, pp. 1215–1224, 2020.
- Song, C., Lin, Y., Guo, S., and Wan, H. Spatial-temporal synchronous graph convolutional networks: A new framework for spatial-temporal network data forecasting. In *The Thirty-Fourth AAAI Conference on Artificial Intelligence*, pp. 914–921, 2020.
- Sutskever, I., Vinyals, O., and Le, Q. V. Sequence to sequence learning with neural networks. *Advances in neural information processing systems*, 27, 2014.
- Tedjopurnomo, D. A., Bao, Z., Zheng, B., Choudhury, F., and Qin, A. K. A survey on modern deep neural network for traffic prediction: Trends, methods and challenges. *IEEE Transactions on Knowledge and Data Engineering*, 2020.
- Vaswani, A., Shazeer, N., Parmar, N., Uszkoreit, J., Jones, L., Gomez, A. N., Kaiser, Ł., and Polosukhin, I. Attention is all you need. *Advances in neural information processing systems*, 2017.
- Velickovic, P., Cucurull, G., Casanova, A., Romero, A., Lio, P., and Bengio, Y. Graph attention networks. *stat*, 1050: 20, 2017.
- Wang, X., Ma, Y., Wang, Y., Jin, W., Wang, X., Tang, J., Jia, C., and Yu, J. Traffic flow prediction via spatial temporal graph neural network. In *WWW '20: The Web Conference 2020*, pp. 1082–1092, 2020.
- Woo, S., Park, J., Lee, J.-Y., and Kweon, I. S. Cbam: Convolutional block attention module. In *Proceedings of the European conference on computer vision (ECCV)*, pp. 3–19, 2018.
- Wu, C., Ho, J., and Lee, D. Travel-time prediction with support vector regression. *IEEE Trans. Intell. Transp. Syst.*, pp. 276–281, 2004.
- Wu, Z., Pan, S., Long, G., Jiang, J., and Zhang, C. Graph wavenet for deep spatial-temporal graph modeling. *arXiv preprint arXiv:1906.00121*, 2019.
- Wu, Z., Pan, S., Long, G., Jiang, J., Chang, X., and Zhang, C. Connecting the dots: Multivariate time series forecasting with graph neural networks. In *Proceedings of the 26th ACM SIGKDD international conference on knowledge discovery & data mining*, pp. 753–763, 2020.
- Xu, M., Dai, W., Liu, C., Gao, X., Lin, W., Qi, G.-J., and Xiong, H. Spatial-temporal transformer networks for traffic flow forecasting. *arXiv preprint arXiv:2001.02908*, 2020.
- Yao, H., Tang, X., Wei, H., Zheng, G., and Li, Z. Revisiting spatial-temporal similarity: A deep learning framework for traffic prediction. In *Proceedings of the AAAI conference on artificial intelligence*, pp. 5668–5675, 2019.
- Yu, B., Yin, H., and Zhu, Z. Spatio-temporal graph convolutional networks: A deep learning framework for traffic forecasting. In *Proceedings of the Twenty-Seventh International Joint Conference on Artificial Intelligence*, pp. 3634–3640, 2018.
- Zhang, J., Zheng, Y., and Qi, D. Deep spatio-temporal residual networks for citywide crowd flows prediction. In *Thirty-first AAAI conference on artificial intelligence*, 2017.
- Zhao, L., Song, Y., Zhang, C., Liu, Y., Wang, P., Lin, T., Deng, M., and Li, H. T-GCN: A temporal graph convolutional network for traffic prediction. *IEEE Trans. Intell. Transp. Syst.*, pp. 3848–3858, 2020.
- Zheng, C., Fan, X., Wang, C., and Qi, J. GMAN: A graph multi-attention network for traffic prediction. In *The Thirty-Fourth AAAI Conference on Artificial Intelligence*, pp. 1234–1241, 2020.

A. Appendix: Related Work

Traffic road network is a complex dynamical system with temporal and spatial properties. In recent years, spatio-temporal graph neural networks (STGNNs) have shown dominant performance in traffic prediction tasks. It is natural to combine graph convolution networks and sequence models to jointly model the spatial and temporal dependence of traffic data. Here we analyze and summarize the common modeling approaches for spatio-temporal graph networks from both temporal and spatial perspectives.

Temporal Dependence Modeling: Temporal convolution networks (TCNs) and recurrent neural networks (RNNs) are widely used to capture the dependencies of time series. Among them, RNNs(LSTM, GRU) (Hochreiter & Schmidhuber, 1997; Chung et al., 2014) can naturally capture the sequential relationships before and after sequences, but require relatively high computational cost. TCNs (Bai et al., 2018) attempt to use 1D convolution to improve computational efficiency, but the implicit time step fixation sacrifices some flexibility. The forgotten gating of RNNs and the fixed convolution kernel of TCNs make it difficult for them to capture long-term temporal relationships. Inspired by self-attention (Vaswani et al., 2017) and its variants on language models surpassing RNNs, many works (Xu et al., 2020; Wang et al., 2020) have proposed to successfully capture long-range temporal dependencies using Transformer layers or self-attention mechanisms. Moreover, AutoEncoder (Kieu et al., 2019) provides a sequence-to-sequence design architecture that encodes sequence information as an embedding layer and then decodes the embedding of the hidden layer as the prediction result. These temporal components provide the theoretical basis for modeling the temporal relationships for traffic forecasting.

Spatial Dependence Modeling: Early research ideas are to divide a region into grids of the same size. ST-ResNet (Zhang et al., 2017) first proposes to use deep residual convolution networks to extract spatial features. Similar works include DeepSTN+ (Lin et al., 2019) and ST-3DNet (Guo et al., 2019b), which model traffic prediction as data processing with an image or video structure. However, this way cannot be accurate to the traffic conditions of a particular road or point. In practice, the topology of traffic road networks is often an irregular non-Euclidean space and CNNs cannot handle such structures. A promising approach is to use graph neural networks (GCN (Kipf & Welling, 2016), GAT (Velickovic et al., 2017), etc.) to learn a high-dimensional space feature representation of the node (Jiang & Luo, 2022). Spatial information is often dynamic and diverse, and many graph-theoretic approaches have been migrated to solve spatial dependence modeling in traffic forecasting. For example, random walk, diffusion convolution (Li et al., 2018) and MixHop (Abu-El-Haija et al., 2019)

are used to learn spatial features with directed, multi-range spatial features. The design of multi-attribute graph design and adaptive graph learning are used to improve the spatial modeling performance of graph convolution networks. In addition, the spatial relationships that change dynamically over time can be effectively represented by the spatial attention between nodes.

Spatial-temporal Graph Neural Network: Spatio-temporal graph neural networks (STGNNs) not only capture the intrinsic time-varying relationships of each variable but also can model the dependencies between variables. In order to improve the capability of spatio-temporal components to capture features, it is necessary to design robust network frameworks. For example, DCRNN (Li et al., 2018) incorporates GRU and diffusion convolution into the Encoder-Decoder architecture. Graph WaveNet (Wu et al., 2019) uses stacked multilayer gated temporal convolution with GCN units. GMAN (Zheng et al., 2020), STTNs (Xu et al., 2020) and ASTGNN (Guo et al., 2021) apply networks with alternative series of spatio-temporal attention. Due to spatial connectivity is dynamically changing rather than fixed, pre-defined graphs are difficult to characterize complete spatial relationships. AGCRN (Bai et al., 2020), MTGNN (Wu et al., 2020), DMSTGCN (Han et al., 2021a) propose parameter learning graph structures to accommodate dynamically changing spatial connectivity relationships. This approach allows mining the underlying spatial information from the features themselves without resorting to external data (e.g., weather, POI, road structure), which is often inaccessible in the real world. The representative spatio-temporal graph neural network methods in recent years are listed in Table 5.

B. Missing Details in the Experiments

Evaluation Metrics. To evaluate the prediction performance of different methods, we select MAE, RMSE, and MAPE as evaluation metrics. RMSE and MAE are used to measure the error between the ground truth of the sample and the predicted result, reflecting the model's fitting accuracy to the real sample, MAPE provides a benchmark for easy comparison, and when the predicted result is the same as the ground truth, MAPE tends to 0. The mathematical definitions of three evaluation metrics are as follows:

- Mean Absolute Error (MAE):

$$MAE = \frac{1}{N} \sum_{i=1}^N |y_i - \hat{y}_i| \quad (18)$$

- Root Mean Squared Error (RMSE):

$$RMSE = \sqrt{\frac{1}{N} \sum_{i=1}^N (y_i - \hat{y}_i)^2} \quad (19)$$

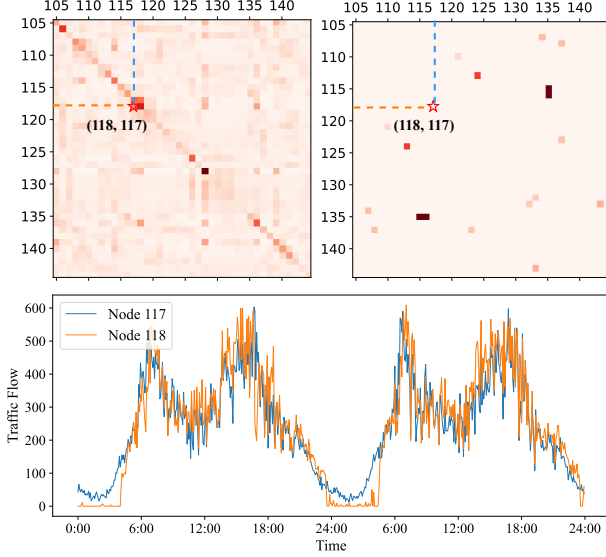


Figure 7. Heatmap visualization for Dynamic Graph (Left) and Pre-defined Graph (Right) in PeMSD4

- Mean Absolute Percentage Error (MAPE):

$$MAPE = \frac{100\%}{N} \sum_{i=1}^N \left| \frac{y_i - \hat{y}_i}{y_i} \right| \quad (20)$$

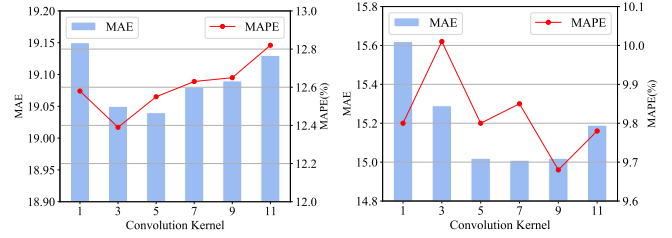
For the MAE, RMSE, and MAPE metrics, smaller values indicate better prediction performance.

Parameters Setup. We set uniform model parameters on four datasets with the hidden dimension of 64, head of attention of 4, order of graph convolution of 2, batch size of training samples of 64, and learning rate of the model of 0.003. In addition, the model has two main hyperparameters including Embedding Dimension in $\{2, 4, 6, 8, 10, 12\}$, and 1D Convolution Kernel in $\{1, 3, 5, 7, 9, 11\}$. To achieve the best performance of the model, we set the Embedding Dimension and the 1D convolution kernel differently in different datasets, 4 and 5 in PeMSD3, 8 and 5 in PeMSD4, 6 and 5 in PeMSD7, and 4 and 9 in PeMSD8. The supplementary experimental results of the model evaluation are shown in Table 6 and Fig. 9.

Interpretability. Now we provide a shred of evidence on the benefit of using an adaptive graph structure. We visualize the correlation between every node pair under dynamic and pre-defined graphs using heatmaps on the PeMSD4 dataset, as shown in Fig. 7. The darker the color, the stronger the correlation between the nodes. The pre-defined graph (right) relies only on geographic distances and does not reflect the complete spatial information of the road network. The information in the pre-defined graph presented by the heatmap is sparse and single. The dynamically generated graph for parameter learning (left) can fully express the dynamics among the nodes in the graph. The information displayed by the heatmap is dense and diverse. We take

two points in the road network as an example (as shown by the star in the figure), which do not exhibit correlation in the pre-defined static graph. But in fact, the two points (Node 117, Node 118) are very close to each other in terms of the period and trend changes of traffic as in the bottom figure. In contrast, our dynamically generated graph can reflect this clearly. Therefore, the dynamic adjacency matrix can implicitly learn the dynamic representation of the road network and provide an effective complement to the static adjacency matrix.

Moreover, we also present the MAE/RMSE in each prediction step of AFDGCN and the four variants in Fig. 9. We observe that AFDGCN consistently outperforms DGCGRU, (DGC-ATT)DGCGRU with ATT, AFDGCN w/o GAT, and AFDGCN w/o AF, indicating the effectiveness of temporal attention, spatial attention, and feature augmentation in modeling complex spatio-temporal correlations.



(a) Kernel Size in PeMSD4 (b) Kernel Size in PeMSD8

Figure 8. The Effects of Convolution Kernel Size

Another hyperparameter study. Among the model parameters, the size of the temporal convolution kernels for feature augmentation also has an impact on the performance of the model. As shown in Figures 8(a) and 8(b), in general, the best convolution kernel size in the PeMSD4 and PeMSD8 datasets are 3 and 9. When calculating the temporal weight sum in the feature augmentation layer, a very small convolution kernel size could limit the perceptual field of the features, while a very large kernel size could distract from the sequence length. In practice, one can tune the kernel size to achieve a good model performance.

Table 5. Spatial-Temporal Graph Neural Networks in traffic prediction.

Method	Spatial Modeling			Temporal Modeling			Method	Spatial Modeling			Temporal Modeling		
	SGCN	DGCN	S-Att	TCN	RNN	T-Att		SGCN	DGCN	S-Att	TCN	RNN	T-Att
STGCN (Yao et al., 2019)	✓			✓			MRA-BGCN (Chen et al., 2020)	✓		✓		✓	
GWNET (Wu et al., 2019)	✓	✓		✓			STGODE (Fang et al., 2021)	✓			✓		
T-GCN (Zhao et al., 2020)	✓				✓		ST-GRAT (Park et al., 2020)			✓			✓
DCRNN (Li et al., 2018)	✓				✓		ASTGCN (Guo et al., 2019a)	✓		✓			✓
GMAN (Zheng et al., 2020)			✓			✓	DSTAGNN (Lan et al., 2022)		✓	✓			✓
ASTGNN (Guo et al., 2021)	✓		✓			✓	AGCRN (Bai et al., 2020)		✓			✓	
STGNN (Wang et al., 2020)	✓		✓		✓	✓	DGCRN (Li et al., 2021)		✓			✓	
STTNs (Xu et al., 2020)	✓		✓			✓	MTGNN (Wu et al., 2020)		✓		✓		
LSGCN (Huang et al., 2020)	✓		✓	✓			DMSTGCN (Han et al., 2021b)		✓		✓		

¹ SGCN denotes GCN based on static graph structure.

² DGCN denotes GCN based on the dynamic generation of the graph.

Table 6. Performance comparison of AFDGCN and other baseline models. AFDGCN achieves the best performance for all datasets.

Model	PEMSD3			PEMSD4			PEMSD7			PEMSD8		
	MAE	RMSE	MAPE	MAE	RMSE	MAPE	MAE	RMSE	MAPE	MAE	RMSE	MAPE
FC-LSTM	21.33	35.11	23.33%	26.77	40.65	18.23%	29.98	45.94	13.20%	23.09	35.17	14.99%
TCN	19.32	33.55	19.93%	23.22	37.26	15.59%	32.72	42.23	14.26%	22.72	35.79	14.03%
TCN(w/o causal)	18.87	32.24	18.63%	22.81	36.87	14.31%	30.53	41.02	13.88%	21.42	34.03	13.09%
GRU-ED	19.12	32.85	19.31%	23.68	39.27	16.44%	27.66	43.49	12.20%	22.00	36.22	13.33%
DSANet	21.29	34.55	23.21%	22.79	35.77	16.03%	31.36	49.11	14.43%	17.14	26.96	11.32%
MSTGCN	19.54	31.93	23.86%	23.96	37.21	14.33%	29.00	43.73	14.30%	19.00	29.15	12.38%
STG2Seq	19.03	29.83	21.55%	25.20	38.86	13.18%	32.77	47.16	20.16%	20.17	30.71	17.32%
LSGCN	17.94	29.85	16.98%	21.53	33.86	13.18%	27.31	41.46	11.98%	17.73	26.76	11.20%
STFGNN	16.77	28.34	16.30%	20.48	32.51	16.77%	23.46	36.60	9.21%	16.94	26.25	10.60%
AFDGCN	14.97	25.81	14.18%	19.09	31.01	12.62%	20.22	33.80	8.52%	15.02	24.37	9.68%

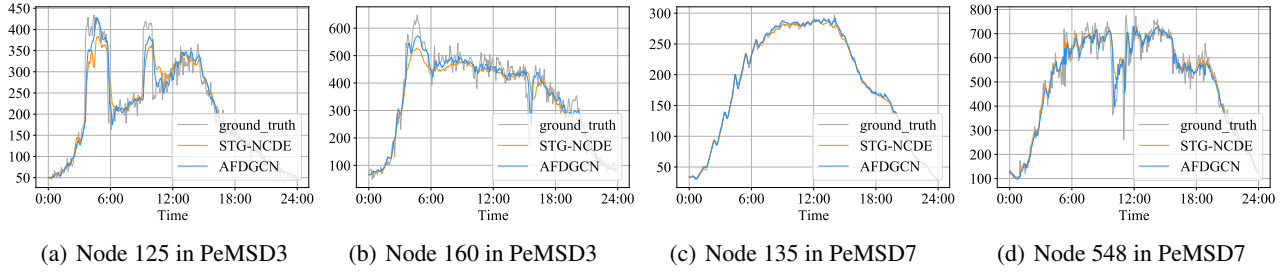


Figure 9. Traffic forecasting visualization at different time points in PEMS3 and PEMS7

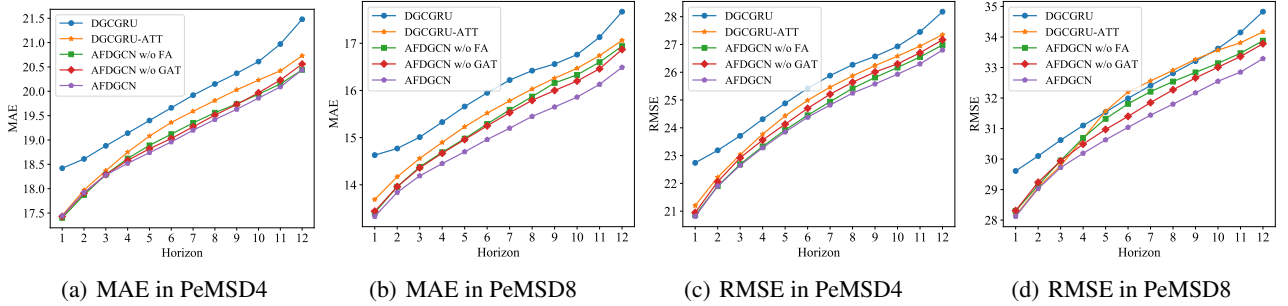


Figure 10. MAE and RMSE of each prediction step